Clim Dyn (2015) 44:791–806
DOI 10.1007/s00382-014-2139-z

Probabilistic reconstructions of local temperature and soil moisture from tree-ring data with potentially time-varying climatic response

S. E. Tolwinski-Ward · M. P. Tingley · M. N. Evans · M. K. Hughes · D. W. Nychka

Received: 26 August 2013 / Accepted: 8 April 2014 / Published online: 29 April 2014

Abstract We explore a probabilistic, hierarchical Bayesian approach to the simultaneous reconstruction of local temperature and soil moisture from tree-ring width observations. The model explicitly allows for differing calibration and reconstruction interval responses of the ring-width series to climate due to slow changes in climatology coupled with the biological climate thresholds underlying tree-ring growth. A numerical experiment performed using synthetically generated data demonstrates that bimodality can occur in posterior estimates of past climate when the data do not contain enough information to determine whether temperature or moisture limitation controlled reconstruction-interval tree-ring variability. This manifestation of nonidentifiability is a result of the many-to-one mapping from bivariate climate to time series of tree-ring widths. The methodology is applied to reconstruct temperature and soil moisture conditions over the 1080–1129 C.E. interval at Methusalah Walk in the White Mountains of California, where co-located isotopic dendrochronologies suggest that observed moisture limitations on tree growth may have been alleviated. Our model allows for assimilation of both data sources, and computation of the probability of a change in the climatic controls on ring-width relative to those observed in the calibration period. While the probability of a change in control is sensitive to the choice of prior distribution, the inference that conditions were moist and cool at Methuselah Walk during the 1080–1129 C.E. interval is robust. Results also illustrate the power of combining multiple proxy data sets to reduce uncertainty in reconstructions of paleoclimate.

Keywords Bayesian hierarchical modeling · Biological–statistical modeling · Multiproxy paleoclimate reconstruction · Tree-ring width · Time-varying climate-paleodata relationship

Electronic supplementary material The online version of this article (doi:10.1007/s00382-014-2139-z) contains supplementary material, which is available to authorized users.

S.E. Tolwinski-Ward performed the research and submitted the article while at the Institute for Mathematics Applied to Geosciences, National Center for Atmospheric Research, Boulder, CO, 80305.

S. E. Tolwinski-Ward (✉)
AIR Worldwide Corporation, Boston, MA 02116, USA
e-mail: suzski@gmail.com

M. P. Tingley
Department of Meteorology and Statistics, Pennsylvania State University, University Park, PA 16802, USA

M. N. Evans
Department of Geology, University of Maryland, College Park, MD 20742, USA

M. K. Hughes
Laboratory of Tree-Ring Research, University of Arizona, Tucson, AZ 85721, USA

D. W. Nychka
Institute for Mathematics Applied to Geosciences, National Center for Atmospheric Research, Boulder, CO 80305, USA

1 Introduction

Time series of tree-ring widths (TRWs) provide one of the best-dated and most spatially extensive records of paleoclimatic variability (Jansen et al. 2007), and most attempts to reconstruct climate at global or hemispheric scales rely heavily upon them (Jones et al. 1998; Crowley and Lowery 2000; Moberg et al. 2005; D'Arrigo et al. 2006; Mann et al. 2008; Christiansen and Ljungqvist 2011). Such reconstructions are often based on establishing linear, empirical–statistical relationships between the paleo-observations and

a single climatic variable during a calibration period, and assuming the climate-paleodata relationship applies in earlier times without modification. Researchers have long recognized that the latter assumption, known as 'the principle of uniformitarianism' (Bradley 1999, p. 4), should be tested (e.g. Hughes and Ammann 2009), especially when past values of the climatic drivers of the paleodata may have been outside the range observed in the calibration period. Such tests require methods that deal explicitly with changes in the response by modeling the causal effect of a changing environment on the proxy archive, rather than treating the data as if they were produced by using thermometers or rain gauges.

Inferring climate from ring-width data is challenging because trees are fundamentally lossy recorders of climate. Information about the climatic conditions at the time of growth is lost in part because growing trees integrate subannually-resolved climatic conditions (Bradley 2011), and because ring-width chronologies are standardized to remove non-climatic effects on growth (Cook and Kairiukstis 1990). A larger source of information loss arises from the joint influence of both temperature and moisture on tree growth. Without assuming that a site's climatology was the same in the past as during instrumentally observed times, it is impossible to attribute tree ring width variability to variations in one climatic variable or the other. In mathematical terms, the transformation from the space of all possible climate histories to the space of tree-ring with series is not one-to-one. This hallmark feature of inverse problems means that regularization, or the incorporation of information from an informative prior or an additional type of observation, is required to enable mathematical solution.

In traditional regression-based climate reconstructions, the problem is implicitly regularized by restricting analysis to sets of data that roughly conform to the assumption of a linear and stationary relationship between ring width and univariate climate. Indeed, site-selection techniques have been developed in dendrochronology to maximize the chances that the signal contained in ring-width samples is univariate (Stokes and Smiley 1968; Cook and Kairiukstis 1990. While this traditional approach yields a statistically straightforward solution, it sacrifices more nuanced, mechanisms-based information about paleodata formation. In particular, paleoobservations that originate from an evolving and/or nonlinear proxy system response to environmental forcing may bias reconstruction and uncertainty estimates derived by assuming a static and/or linear response.

Here we develop, test, and apply a Bayesian hierarchical model for inferring past climate, based on a mechanistic understanding of the tree ring response to soil moisture and temperature variability. Bayesian hierarchical models (BHMs) permit a fundamentally different solution to the inverse problem, and are powerful and well-established tools in the statistical sciences (Gelman et al. 2003). Similar tools have recently been proposed (Hughes and Ammann 2009; Tingley et al. 2012) and used (Li et al. 2010; Tingley and Huybers 2010a, b, 2013; Haslett et al. 2006; Wahl et al. 2011; Guiot et al. 2009; Parnell et al. 2008; Yu et al. 2012; Garetta et al. 2012) for aspects of paleoclimate reconstructions. This inference framework enables coupling of forward models of the lossy ring-width formation process to stochastic models of climate. "Inverting" the mechanistically based forward models using Bayes' law can then provide a different avenue for regularizing the reconstruction problem and lending increased scientific interpretability to results (Guiot et al. 2000; Hughes and Ammann 2009). In particular, use of a validated forward model of tree-ring width growth that models the potential of the biological system to change its response to climate may provide a more defensible interpretation of ring-width data. Within the Bayesian framework, the relative probabilities of distinct climate histories that map to the same paleodata series under the forward model are weighted according to a formal model for the prior information about the site climatology.

We develop a Bayesian hierarchical model that employs a mechanisms-based forward model of tree-ring growth to tie the data to past variations in temperature and soil moisture (Sect. 2). For a limited range of climatic inputs, the model can produce synthetic tree-ring responses that appear linear and univariate, but for more widely varying climatic time series, it can produce switching in the response of paleodata from temperature to soil moisture or vice versa. The forward model can thus be viewed as a more general representation of tree-ring growth that subsumes models expressing ring width as a linear function of univariate climate. In the inverse reconstruction problem, this forward response-switching capability manifests itself in non-Gaussian, bimodal posterior probability densities, which we explore in a controlled "pseudoproxy" reconstruction experiment (Sect. 3). We use synthetic target climate series and simulated tree-ring data engineered such that the climatic controls on the data are known to differ in the calibration- and reconstruction-intervals.

We use the same approach to infer pre-instrumental climate from Methuselah Walk, a site close to the lower elevational limit of Great Basin bristlecone pine (*Pinus longaeva* DK Bailey) in the White Mountains of California (Sect. 4). The ring-width data from this specific site are known to be primarily indicative of local moisture variability (Hughes and Funkhouser 1998), but isotopic data from trees at the same site indicate that a 50-year medieval interval was anomalously wet (Leavitt 1994). In this real-data context, the goal of our research is threefold. First, we seek an estimate of the paleoclimatology of the interval 1080–1129 AD that accounts for the possibility that the past ring-width signal may contain information about

temperature or about soil moisture. Secondly, we wish to elucidate the importance of prior information on the inference when a more general model of proxy response to climate is used to interpret the tree-ring data. Finally, we explore the utility of an additional source of proxy information, in this case isotope dendrochronologies, to reduce reconstruction uncertainty when the ring-width indices are allowed to be interpreted more broadly than as a linear function of univariate climate. We end with discussion and conclusions (Sect. 5).

2 A hierarchical model for climate and tree ring widths

In what follows, we use the notation $[X]$ to denote the probability density of the random variable X and $[X|Y]$ to denote the density of X conditioned on Y. Model-building using BHMs proceeds by first specifying a probabilistic model for the state variables of interest, called the *process level* and denoted $[X|\theta_X]$, where X is the process of interest and θ_X is a parameter or set of parameters on which the prior model may depend. A *data-level model* $[Y|X,\theta_Y]$ describes the dependence of the data Y on X, and includes a set of data-level model parameters θ_Y. In the Bayesian framework, the parameters of the data- and process-level models are also given random interpretation and *parameter-level* prior distributions $[\theta_X]$ and $[\theta_Y]$. The object of our analysis is the *posterior distribution* $[X,\theta_X,\theta_Y|Y]$, the joint distribution of the process of interest and model parameters conditional on the data, and is defined through Bayes' law:

$$[X,\theta_X,\theta_Y|Y] \propto [Y|X,\theta_Y][X|\theta_X][\theta_X][\theta_Y] \quad (1)$$

The properties of the posterior distribution are generally determined by numerically generating samples from the posterior distribution via Monte Carlo analysis.

In the present context, the data level models the vector of tree-ring width index data $\boldsymbol{W}$ as dependent on vectors of temperature $\boldsymbol{T}$ and soil moisture $\boldsymbol{M}$, with parameters $\boldsymbol{\theta}_W$. The process level specifies a stochastic representation of $\boldsymbol{T}$ and $\boldsymbol{M}$, parameterized by $\boldsymbol{\theta}_{T,M}$, while the parameter level provides numerical closure by specifying priors for $\boldsymbol{\theta}_{T,M}$ and $\boldsymbol{\theta}_W$. We further assume that ring width is conditionally independent of the process-level parameters given realizations of the process-level variables, and that the data- and process-level parameters are independent. Bayes' Law then takes the form

$$[\boldsymbol{T},\boldsymbol{M},\boldsymbol{\theta}_W,\boldsymbol{\theta}_{T,M}|\boldsymbol{W}] \propto [\boldsymbol{W}|\boldsymbol{T},\boldsymbol{M},\boldsymbol{\theta}_W][\boldsymbol{T},\boldsymbol{M}|\boldsymbol{\theta}_{T,M}][\boldsymbol{\theta}_W][\boldsymbol{\theta}_{T,M}]. \quad (2)$$

A schematic diagram of the relationships between variables is given in Fig. 1, while a list of variables and the specific components of the parameter vectors is given in Table 1. Two separate time scales are necessary, as the tree-ring-width data are annually-resolved, but the climate variables are represented at monthly resolution. Let $s = 1,2,\ldots 12$ index the month in any given year, and let $t = 1,2,\ldots,T$ index the years corresponding to tree-ring-width data. Monthly resolved process variables are the indexed by the pair (s,t), while annually resolved variables are indexed only by t. The following subsections describe the data-level (2.1) model, the joint process-level model for the climate (2.2), the priors for the parameters (2.3).

Table 1 Model variables and parameters

Data-Level Variable	
$W(t)$	Ring-width index (unitless, annual resolution)
Data-level parameters (parameters of VS-Lite)	
T_1, T_2	Threshold temp. for nonzero and optimal growth, resp. (°C)
M_1, M_2	Threshold soil moist. for nonzero and optimal growth, resp. (v/v)
σ_w^2	Variance of data model noise (unitless)
Process-level variables	
$T(s,t)$	Temperature (°C, monthly resolution)
$M(s,t)$	Soil Moisture (v/v, monthly resolution)
Process-level parameters	
ΔT, ΔM	Mean shifts in T, M climatology (calibr. interval std. deviations)
Hyperparameters	
$\mu_T(s)$	Mean temperature in month s (°C)
$\sigma_T^2(s)$	Temperature variance in month s (°C^2)
$(\alpha_M(s),\beta_M(s))$	Soil moisture shape parameters in month s (unitless)
(M_n,M_x)	Minimum and maximum allowable soil moisture values (v/v)
S_s	Covariance matrix for temperature and soil moisture in month s
(ϕ_1,ϕ_2)	AR(1) parameters underlying temporal structure of climate (unitless)

2.1 Modeling the data level variable

The time series of ring-width indices that we take as our starting point is two steps removed from raw measurements. Generally 'site chronologies' are derived from the combination of many replicated measurements from multiple co-located trees, with repeated samples taken from each tree. In this case we used such a mean series for the Methuselah Walk location. It was developed by D.A. Graybill and is available as record CA535 obtained from the International Tree-Ring Data Bank, as are the raw measurements from which it was calculated.[1] In order to

[1] http://hurricane.ncdc.noaa.gov/pls/paleox/f?p=519:1:::::P1_STUDY_ID:3376.

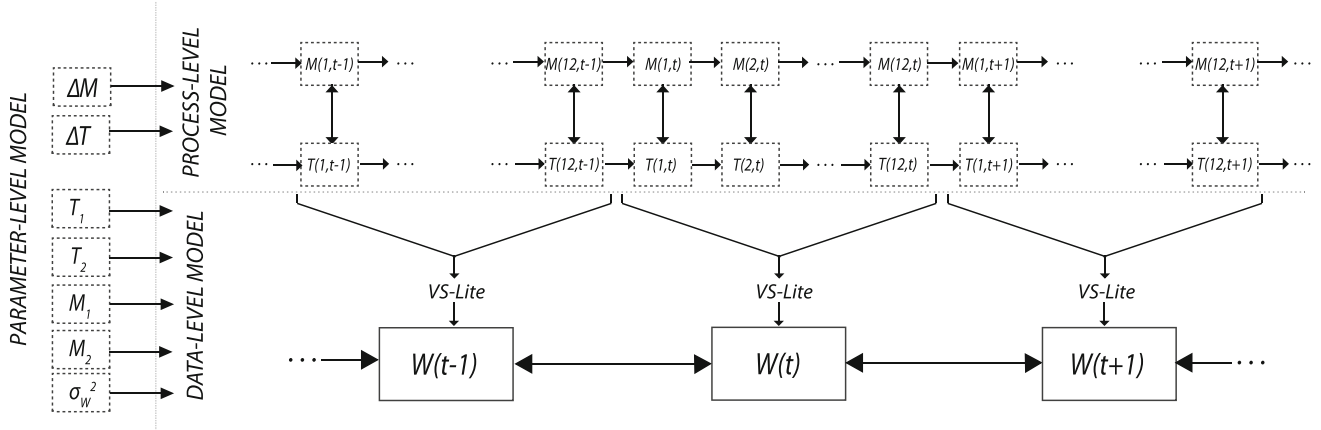

Fig. 1 Structure of the Bayesian hierarchical model developed in Sect. 2 to reconstruct monthly temperature T and moisture M from observed annual tree-ring width W. Random variables are outlined in *dashed boxes*, and fixed variables are outlined in *solid boxes*. The directions of the *arrows* represent the directions of conditional dependencies between variables. Note that the *arrows* between annual ring-width indices $W(t)$ reflect the interdependence of these values due to the time series standardization

remove non-climatic variation in ring width associated with tree size or age, each sample's annual ring-width series was detrended. This was done by fitting a negative exponential curve or a straight line of zero or negative trend and then deriving dimensionless tree-ring width indices by dividing the actual ring-width by that year's value for the fitted line. These individual sample tree ring-width indices were then averaged to form the site chronology. There were at least 31 samples represented for every year of the period of interest in this case (1080–1129 C.E.). Stokes and Smiley (1968) and Cook and Kairiukstis (1990) provide further background on the development of dendrochronologies. While others have worked toward explicit statistical models of the chronology from raw measurements,[2] here we use the derived series and neglect any sources of error deriving from the data processing.

The data-level model is based on the Vaganov–Shashkin-Lite (VS-Lite) model, which has been shown to successfully simulate climatic influences on tree growth and output realistic simulated site dendrochronologies (Shashkin and Vaganov 1993; Vaganov et al. 2006; Tolwinski-Ward et al. 2011; Breitenmoser et al. 2013). VS-Lite provides a simple yet scientifically motivated model of climate-driven tree-ring width as a function of monthly temperature and moisture, and so its use at the data level here represents a forward model "inversion" for paleoclimate estimation (Guiot et al. 2000; Hughes and Ammann 2009; Evans et al. 2013). At each model timestep, indexed by month s and year t, scaled growth responses $g_T(s,t)$ and $g_M(s,t)$ between zero and one are associated with temperature and soil moisture, respectively. Defining the piecewise "standard ramp" function $\Psi(u)$ as,

$$\Psi(u) = \begin{cases} 0 & \text{for} \quad u \leq 0 \\ u & \text{for} \quad 0 < u < 1 \\ 1 & \text{for} \quad u \geq 1, \end{cases}$$

the growth responses $g_T(s,t)$ and $g_M(s,t)$ are given by

$$g_T(s,t) = \Psi\left(\frac{T(s,t) - T_1}{T_2 - T_1}\right) \tag{3}$$

$$g_M(s,t) = \Psi\left(\frac{M(s,t) - M_1}{M_2 - M_1}\right). \tag{4}$$

Equations (3) and (4) introduce an important nonlinearity by setting thresholds below which a tree will not grow at all (T_1 and M_1), and thresholds above which warmer or wetter conditions will not increase growth (T_2 and M_2). An additional scaled growth response to insolation, $g_E(s)$, is a scaling of the mean daylength in each month to the unit interval, and is used in the model as a proxy for insolation. The overall growth response $\Gamma(t)$ for each year is then,

$$\Gamma(t) = \sum_s g_E(s) \cdot \min\{g_T(s,t), g_M(s,t)\}. \tag{5}$$

The minimum in Eq. 5 represents a second nonlinearity not typically represented in traditional reconstructions of climate. This model feature is meant to mimic the Principle of Limiting Factors, which states that tree ring growth is constrained by the environmental variable that is most limiting (Fritts 2001). The minimum endows the model with a "switching" ability, in which the response to climate in a given month may be controlled by either temperature or soil moisture depending on their relative values. The sum over months integrates subannual climatic

[2] M. Schofield et al., abstract 306105 of the 2012 Joint Statistical Meetings.

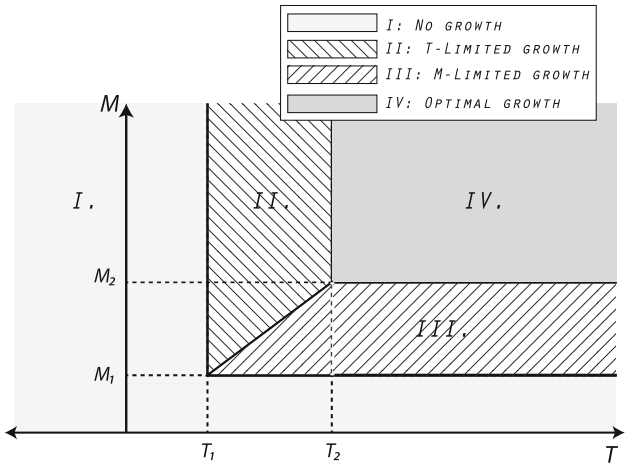

Fig. 2 The growth response simulated for each monthly time step by VS-Lite depends where the climate falls within the joint space of temperature and soil moisture relative to the growth response parameters

influences on growth over the growing season on the modeled signal. The resulting series $\{\Gamma(t), t = 1, 2, \ldots, T\}$ is standardized over the T simulation years to produce a simulated ring width index series $\hat{\boldsymbol{W}}_{VSL}$ comparable with observed standardized chronologies over the same time interval. The VS-Lite model has been validated for a range of sites across North America (Tolwinski-Ward et al. 2011) as well as globally (Breitenmoser et al. 2013).

We then form the data-level model as a scaling of the deterministic VS-Lite output plus independent Gaussian noise. The error term characterizes the combined effects of observational error and model inadequacy, and the form of the error model is supported by preliminary analysis of the model fit to observed data used in this study. Letting vectors $\boldsymbol{T}$ and $\boldsymbol{M}$ represent the monthly-resolved temperature and soil moisture inputs, the data-level model is,

$$\boldsymbol{W}|\boldsymbol{T}, \boldsymbol{M}, \boldsymbol{\theta}_W \sim N\left(\sqrt{1-\sigma_w^2}\hat{\boldsymbol{W}}_{VSL}, \sigma_w^2 I\right). \tag{6}$$

The scaling coefficient on the VS-Lite time series, the square root of one minus the variance of the Gaussian white-noise model, reflects the fact that VS-Lite produces a mean-zero, unit variance time series. Thus the sum of the scaled VS-Lite output and the stochastic errors will have the same unit variance as observed ring-width series, which are standardized over the calibration interval (Tolwinski-Ward et al. 2013).

Figure 2 shows the modeled monthly growth response surface as a function of temperature and soil moisture. Region I of climate space is inhospitable for trees, as it is either too cold or too dry for growth to occur. At the other extreme, neither temperature nor moisture limit growth in region IV. In the language of dendroclimatology, trees growing in locations with climatology in this region of state space are "complacent" (Fritts et al. 1965), and dendroclimatologists take precautions not to sample cores from sites expected to produce complacent records. Regions II and III correspond to "responsive" trees, which are deemed to be ideally situated for sampling for dendroclimatology. If the climatology of a modeled site generally places T and M in region II during the peak of the growing season, then the modeled tree-ring growth will be temperature-limited, and the synthetic ring-width chronology will contain a temperature signal. Trees that experience region III climatologies will be moisture limited. The "switching" in proxy system response to climate considered in this paper can be recast in terms of transitions between regions in Fig. 2 induced by slow changes in the base climate.

2.2 Joint modeling of temperature and moisture

The process-level model describes the seasonality, temporal structure, and local covariance of the target temperature and soil moisture, and also accounts for changes in the climate from the calibration interval. The distributions of $T(s,t)$ and $M(s,t)$ for month s and year t are modeled by a strategic transformation of two latent variables with simpler distributions. Temperature in any month is approximately normally distributed, and soil moisture is reasonably well-described by a linearly transformed beta distribution. Thus interannual variations in the two variables may be written as de-seasonalizing transformations of Gaussian anomaly processes T' and M' from the climatology:

$$T'(s,t) = \frac{T(s,t) - \mu_T(s)}{\sigma_T(s)} - \Delta T \tag{7}$$

$$M'(s,t) = \Phi^{-1}\Big(F_s(M(s,t))\Big) - \Delta M. \tag{8}$$

$F_s(\cdot)$ is the cumulative distribution function of a four-parameter beta-distributed argument, with month-specific shape parameters and lower and upper bounds on its support given by the minimum and maximum allowable soil moisture values, and Φ^{-1} is the inverse standard normal cumulative distribution function.

The parameters ΔT and ΔM describe changes in the climatology compared to the calibration interval parameterization, and are treated as random variables. When $\Delta T = \Delta M = 0$, as in the calibration interval itself, the transformation of temperature depends only on seasonally dependent parameters $\mu_T(s)$ and $\sigma_T(s)$, which are given by the sample mean and standard deviation of the monthly calibration-interval temperatures in month s across all calibration-interval years. Likewise, when $\Delta M = 0$, Eq. 8 transforms the four-parameter beta-distributed soil

moisture into the standard-normal M' process via anamorphosis (Chiles and Delfiner 1999, section 6.2). In contrast, nonzero values of ΔT and ΔM shift the mean of the perturbed variables T' and M' away from zero, allowing for climatic conditions that are substantially different from the calibration interval. The presence of these parameters relaxes the often implicitly-made assumption in more traditional reconstructions that the reconstruction interval has the same climatology as that observed in the instrumental period.

We account for covariance between temperature and soil moisture, as well as temporal persistence, by specifying an AR(1) time series model for the deseasonalized climatic anomalies T' and M':

$$\begin{pmatrix} T'(s,t) \\ M'(s,t) \end{pmatrix} \sim N\left(S_s^{1/2} \begin{bmatrix} \phi_1 & 0 \\ 0 & \phi_2 \end{bmatrix} S_{s_-}^{-1/2} \begin{pmatrix} T'_-(s,t) \\ M'_-(s,t) \end{pmatrix}, S_s \right) \tag{9}$$

The subscript "$-$" denotes the value of a variable at the previous monthly time step; the matrix S_s is 2×2 covariance matrix between the two processes in month s; and ϕ_1 and ϕ_2 capture the temporal autocorrelation.

To develop a realistic stochastic description of monthly resolved temperature and soil moisture, we fit the process-level model to the gridded Parameter–Elevation Regressions on Independent Slopes Model (PRISM) data product (Daly et al. 2008). The gridded data product consists of monthly means over the daily recorded minimum temperatures, monthly means over the daily recorded maximum termperatures, and monthly accumulated precipitation, interpolated to 4 km $\times$ 4 km resolution across the continental United States. The model for temperature is fitted on the mean of the two temperature fields. We derive estimates of soil moisture by using PRISM as inputs to the Climate Prediction Center's "Leaky Bucket" monthly time-step model of hydrology (Huang et al. 1996), a physically-based water balance model with Markov structure. Measurement and model error inherent in the PRISM data product and the Leaky Bucket model are both neglected.

We take an empirical Bayes' approach to the process-level parameters, estimating parameters of the transforms, the seasonality, temporal persistence, and covariance of temperature and soil moisture "offline" and holding them fixed thereafter (Robert 2007, section 10.4). We estimate soil moisture parameters using maximum likelihood based on linear transformations to the unit interval of calibration-interval soil moisture computed in month s. We use the sample covariance matrix of deseasonalized time series of temperature and soil moisture anomalies in month s over the calibration interval for S_s, and ϕ_1 and ϕ_2 are least-squares estimates of the AR(1) coefficients.

2.3 Modeling the parameter level variables

The random shifts ΔT and ΔM describe changes in climatology from the calibration interval. They are unitless in the standardized Gaussian space of the anomaly climate variables T' and M', but a unit value of either results in a shift by one standard deviation in the space of physical climate variables T and M. As we are interested in how potential interactions between temperature and soil moisture on the tree-ring-width data may influence the inverse paleoclimate inference, we assume independence of the priors on these two variables, so that any interaction in the posterior will be a function of the VS-Lite data-level model. We model the climatological shifts as normally distributed about zero, corresponding to no change at all from the calibration-interval climatology:

$$\begin{aligned} \Delta T &\sim N(0, \sigma_\Delta^2) \\ \Delta M &\sim N(0, \sigma_\Delta^2) \end{aligned} \tag{10}$$

We note that the prior is informative, in that reconstructed values with magnitude greater than $3\sigma_\Delta$ are very unlikely to occur without strong evidence from the data. In the reconstructions that follow, we explore the sensitivity to the prior variances σ_Δ^2 by carrying out analysis for two different values that have paleoclimate interpretations.

The parameters T_1, T_2, M_1, M_2 of the data-level model are loosely interpretable as temperature and soil moisture thresholds above which growth begins or is no longer sensitive to climatic fluctuations. They are given priors based on current scientific understanding of thresholds for tree growth following Tolwinski-Ward et al. (2013). We use a noninformative uniform prior distribution over the unit interval for the error model variance σ_w^2. Given the scaling of the VS-Lite estimate in the data-level model (Eq. 6), values of σ_w^2 near zero (one) would indicate a tree-ring width series with high (low) signal-to-noise ratio.

3 Reconstruction from synthetic data with time-varying climate response

We first present a numerical experiment to explore the switching behavior of the hierarchical model. Simulated, or "pseudoproxy", tree-ring-width data are constructed such that cool, moist conditions drive temperature-limited growth in the calibration interval, but warmer and drier conditions in the reconstruction interval cause a predominantly moisture-driven signal. The reconstruction experiment explores the climatic inferences that are possible from the model using data near the response space boundaries described by VS-Lite (Fig. 2). This "PseudoProxy Experiment" is hereafter referred to as the PPE.

3.1 Methods and design

We choose process-level parameters (Sect. 2.2) to simulate a location with cool moist climatology, and use the resulting model to simulate a 30-year calibration interval. A 30-year reconstruction interval was also simulated by using the same model but with climate change parameters set to $\Delta T = 1.75, \Delta M = -1.5$, corresponding to warming and drying. Parameters for VS-Lite were chosen such that simulated growth under the synthetic calibration interval is temperature-limited, while moisture-limited growth results for the shifted reconstruction-interval climatology (Fig. 3, top panel). The simulated calibration and reconstruction interval data series are comparable in mean and variability (Fig. 3, lower panels), and so there is no way to tell without further information whether each series is the result of temperature- or moisture-limited growth.

The value of the data-level model noise σ_W^2 was set to 0.5 to give a signal-to-noise ratio of 1, which is considered optimistic for real paleoclimate proxies (Smerdon 2012). The reconstruction was performed with data-level parameters fixed at the values used to generate the pseudoproxy data. The only model parameters inferred are the process-level parameters $\boldsymbol{\theta}_{T,M} = (\Delta T, \Delta M)^T$. We choose the spread of the prior to demonstrate whether the simulated change can be recovered by the model when it is unlikely, but not outside the realm of possibilities allowed by the prior (Eq. 10). To do so we set the prior variance σ_Δ^2 such that the simulated climate change falls outside the contour containing the 75 % most probable climate changes, but is still contained within the contour containing 95 % of the prior probability mass.

Given the knowns and unknowns in the PPE, Eq. 2 becomes

$$[\boldsymbol{T}', \boldsymbol{M}', \Delta T, \Delta M | \boldsymbol{W}] \propto [\boldsymbol{W} | \boldsymbol{T}', \boldsymbol{M}', \Delta T, \Delta M][\boldsymbol{T}', \boldsymbol{M}'][\Delta T][\Delta M]. \tag{11}$$

By testing the case where the data formation process is known exactly and where the data contain minimal non-climatic noise, the experiment is designed to provide an upper bound on the information it is possible to retrieve from the lossy, many-to-one transformation of climate inherent to the tree ring widths.

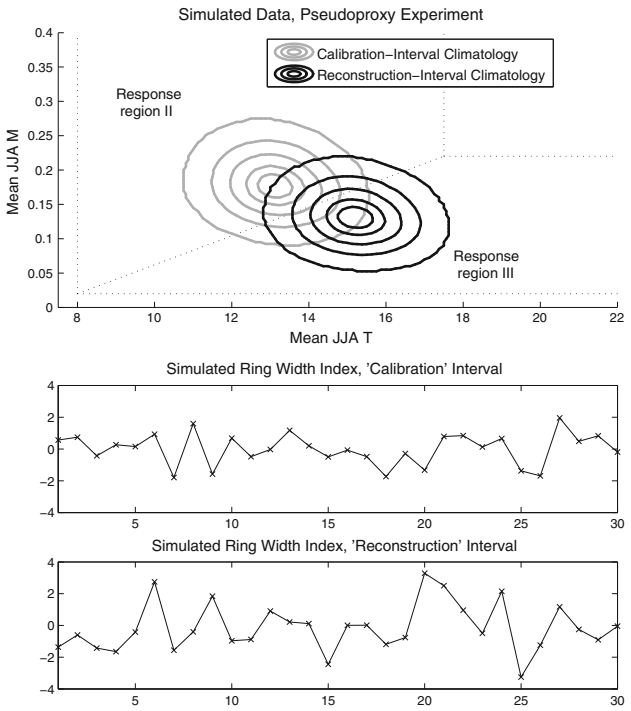

Fig. 3 *Top panel*: Contour plot of the distribution of mean summer moisture and temperature values from Monte Carlo simulations from the calibration and reconstruction interval climatologies in the PPE. The *dotted lines* show the values of the growth threshold parameters used in the experiment, and so delineate the proxy system's "response regions". *Lower two panels*: the simulated calibration and reconstruction interval data series

3.2 Results

The PPE reconstruction consists of a probabilistic ensemble of 2,000 realizations from the posterior distribution of the climate history given the paleodata and data- and process- level model structures (further details of the sampling are given in the "Appendix"). Of principal interest is the posterior reconstruction of the climatic shifts ΔT and ΔM relative to the calibration interval, but we also look at the reconstructed interannual variations in temperature and moisture in order to better interpret our results. Although the reconstruction realizations are resolved at a monthly time-step, the posterior climatic variability could only be meaningfully distinguished at seasonal timescales, reflecting the fact that individual monthly variations are not identifiable from annually-resolved data. We explore the reconstructed interannual variability by looking at the ensemble of means over June, July and August, when the longer relative day lengths result in the bulk of modeled growth.

The joint posterior distribution of ΔT and ΔM, marginalized over monthly $\boldsymbol{T}', \boldsymbol{M}'$, has lesser spread than the prior, implying that conditioning on the synthetic ring-width data has reduced uncertainty about the value of these two parameters (Fig. 4). The true value of the parameters is contained in the 25 % credible region of the posterior distribution, while it lies further toward the edge of the prior (outside of the 75 % credible region, but contained in the 95 % region). Notably, the posterior is bimodal, and has a "boomerang" shape implying a nonlinear relationship between changes in temperature and soil moisture

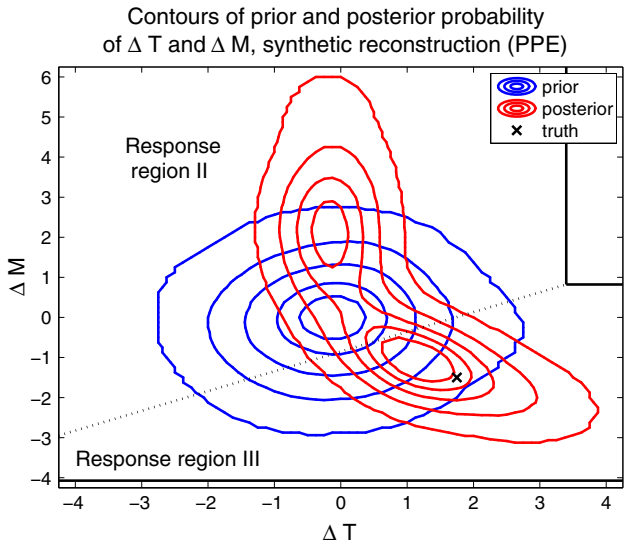

Fig. 4 Contours containing 95, 75, 50, 25, and 10 % of the prior and posterior probability for ΔT and ΔM in the pseudoproxy experiment, along with the true values of the parameters used to generate the synthetic data. Contours are produced using a 2-dimensional kernel-smoother.

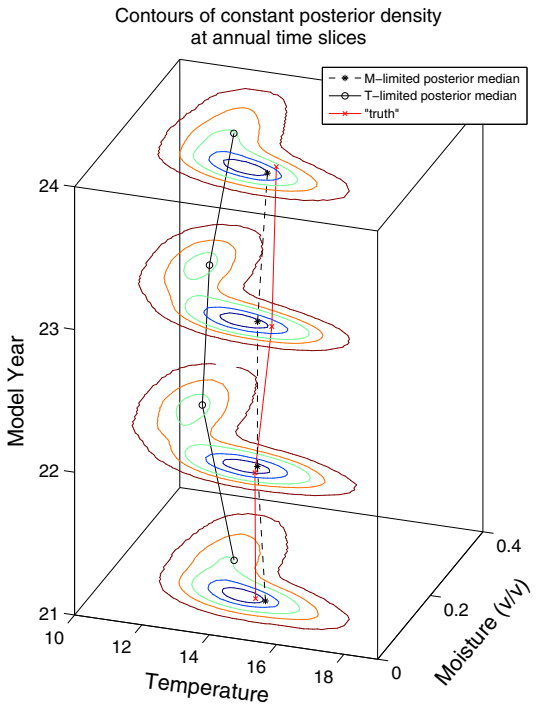

Fig. 5 Plot of contours containing 5, 75, 50, 25, and 10 % of the posterior probability density across four model years in the pseudoproxy experiement. Traces show median of posterior draws of climate inducing moisture-limited simulated growth, median of posterior draws that induce temperature-limited simulated growth, and the "truth", or the time series of simulated climate used to generate the pseudoproxy data. In some years the temperature- and moisture-limited solutions diverge more substantially, creating more defined bimodality in the solution. The estimates of climate that induce moisture-limited simulated tree growth closely track the known bivariate climatic target

climatology that could have produced the reconstruction-interval data.

Separating the posterior realizations of bivariate time series into those that imply differing controls on tree-ring growth can be used to explain the bimodality in the posterior. We classify each climate history by computing the fraction of reconstruction years that fall into each of four categories: (1) the mean summer growth response to temperature is nonzero but less than the growth response to moisture; (2) the growth response to moisture is nonzero but less than the temperature response; (3) both growth responses are one; and (4) both responses are zero. We classify realizations for which these fractions are statistically significantly greater than 0.5 as predominantly temperature-limited, moisture-limited, complacent, or inhospitable for growth, respectively. By this scheme, 41.8 % of the posterior contains temperature-limited climate histories, 48.7 % contains moisture-limited histories, 0 % produce complacent histories, and 0 % produce histories which tended not to grow at all. The remaining 9.5 % of histories had growth which was not dominated by any single control over the reconstructed years. The methodology thus estimates the probability of reconstruction interval climate controls on tree growth that differ from those "observed" during calibration at 58.2 %.

Plotting the contours of posterior probability density for mean summer temperature and soil moisture in time, along with the time series of posterior medians among the temperature-limited and moisture-limited classes of solutions demonstrates the relationship of the controls on growth to the two posterior modes. In some years the temperature- and moisture- limited solutions diverge more substantially than others (e.g. model years 22 and 23 compared to years 21 and 24, Fig. 5), creating more distinct bimodality in the marginal distribution for those years. The temperature- and moisture-limited solutions roughly mirror each other about the line defined implicitly in climate space by equality in the summer mean of the growth responses g_T and g_M. From a mathematical perspective, both sets of climate histories are in the pre-image of the synthetic tree-ring data under the lossy, many-to-one mapping represented by VS-Lite. In other words, both are valid solutions to the inverse problem, and without further information, the model cannot rule out either of the two modes.

4 Multiproxy reconstruction at Methuselah Walk

As a real-world application, we reconstruct the shifts in temperature and soil moisture climatology during the

interval 1080–1129 C.E. using a bristlecone pine ring-width chronology at the Methuselah Walk site in the White Mountains of California (37.26N, −118.10E). This location is characterized by a dry climate, and the Methuselah Walk chronology, which sits more than 700 m below treeline, has positive statistical association with local precipitation and negative association with temperature (Salzer et al. 2009). LaMarche (1974) interpreted tree-ring width records from Methuselah Walk as indicating wet conditions in late eleventh and early twelfth centuries, and also characterized this period as 'warm' based on other material at and near tree-line in the same mountain range. More recently, Salzer et al. (2009) found that the response of bristlecone pine to environmental forcing switches from a negative to a positive relationship with temperature in a zone very close to upper treeline. Based on this result, Salzer et al. (2013) restricted their analysis of past temperatures to tree-ring width data from within 100 m of the contemporaneous upper treeline, and reconstructed colder conditions in the first decades of the twelfth century. We note that the skill of the VS-Lite model at simulating the Methuselah Walk chronology was previously demonstrated by Tolwinski-Ward et al. (2011).

Isotope ratios of $^{13}C/^{12}C$ from the area may also be interpreted as indicators of moisture conditions, and we explore the effects of additionally assimilating this source of information into the reconstruction. In general, depleted (enriched) values of the isotope ratio $\delta^{13}C$ at arid sites are indicative of drier (wetter) conditions (McCarroll and Loader 2004). Leavitt (1994) detrended an isotope chronology from the site to remove low-frequency changes associated with non-climatic variations such as atmospheric isotopic concentration, and found the resulting series was closely tied to moisture conditions. Using this time series, Leavitt (1994) inferred anomalously wet conditions in the period 1080–1129 C.E. The δ^{13}C results of Leavitt (1994) have since been independently replicated and extended to annual resolution at a nearby location, with two clusters of inferred wet years centered on the late 1080s and the early 1120s C.E. (Bale et al. 2011, Fig. 4). We use our hierarchical model to explore the possibility that the moisture controls on ring width growth observed during the calibration interval at Methuselah Walk may have been alleviated during this 1080–1129 C.E. interval due to increased moisture availability.

4.1 Methods and design

In this real-data application, the unknown $\boldsymbol{\theta}_W$ increases both the dimensionality and uncertainty of the problem. Although it is still computationally feasible to reconstruct the annual and subannual climatic variations, we focus on the question of what can be learned about the lower-dimensional shifts in climatology $(\Delta T, \Delta M)$. To explore the dependence of the answer on paleoproxy information, we compare the inferences that can be made from the tree-ring width data and isotopic data separately, and by using the two in combination.

Each reconstruction is also run with two priors distinguished by their variance (σ^2_Δ in Eq. 10) to examine the influence of prior information on the results. The first prior, hereafter called the "7 °C prior", uses a value of the variance parameter such that $\Delta T = \sigma_\Delta$ would result in a local temperature change equal or greater than 7 °C. The 7 °C prior allows for extremely large amplitude climatic change in the context of estimated global Holocene variability, as the upper bound on estimates of global temperature change since the Last Glacial Maximum are roughly 7 °C (Jansen et al. 2007). This prior makes local climatic changes of this magnitude a relatively frequent "1-sigma" event. While the scales of local and global temperature changes differ, the 7 °C prior is designed to demonstrate the effects of prior variance that is large in paleoclimatic terms on the inference from our model. The spread of the second prior is set such that $\Delta T = 2\sigma_\Delta$ would induce a local temperature change in the least variable month at our site of 4.4 °C. To provide a second paleoclimatic benchmark, 4.4 °C is the upper bound on estimates of the temperature change associated with the so-called 8.2 ka event, the most extreme climatic excursion during the Holocene (Kobashi et al. 2007). This second prior represents a more conservative estimate of the potential magnitude of climatological shifts, with local climate change of the magnitude of the 8.2 ka event being a less frequent "2-sigma" event. We refer to this more informative prior as the "2.2 °C prior".

The data-level model for tree-ring width index is unchanged from the PPE. As our focus is on the climatic shifts, we do not directly estimate the monthly temperature and soil moisture anomalies. However, to ensure accurate uncertainty propagation, we integrate over Monte Carlo samples of $\boldsymbol{T}', \boldsymbol{M}'$ from the same process-level model used in the PPE (see "Appendix" for further details). We additionally use calibration interval ring-width data and estimates of temperature and soil moisture derived from calibration-interval instrumental data, together generically denoted as D_{cal}, to put informative priors on the parameters of the data-level model for tree-ring width (c.f. Tolwinski-Ward et al. 2013).

The statement of Bayes rule (Eq. 2) takes one of three forms, depending on the data included in the reconstruction.

1. Isotope data alone:

$$[\Delta T, \Delta M | \overline{I_\delta}, D_{cal}] \propto [\overline{I_\delta} | \Delta M, D_{cal}][\Delta T][\Delta M], \quad (12)$$

2. Tree-ring width alone:

$$[\Delta T, \Delta M, \boldsymbol{\theta}_W | \boldsymbol{W}, D_{cal}] \propto \int [\boldsymbol{W} | \boldsymbol{T}', \boldsymbol{M}', \Delta T, \Delta M, \boldsymbol{\theta}_W] [\boldsymbol{T}', \boldsymbol{M}'] [\Delta T] [\Delta M] [\boldsymbol{\theta}_W | D_{cal}] d\boldsymbol{T}' d\boldsymbol{M}'. \quad (13)$$

3. Both data types:

$$[\Delta T, \Delta M, \boldsymbol{\theta}_W | \boldsymbol{W}, \overline{I_\delta}, D_{cal}] \propto \int [\boldsymbol{W} | \boldsymbol{T}', \boldsymbol{M}', \Delta T, \Delta M, \boldsymbol{\theta}_W] [\boldsymbol{T}', \boldsymbol{M}'] [\Delta T] [\overline{I_\delta} | \Delta M, D_{cal}] [\Delta M] [\boldsymbol{\theta}_W | D_{cal}] d\boldsymbol{T}' d\boldsymbol{M}' \quad (14)$$

In order to formally assimilate the isotopic data I_δ, we develop a simple data-level model for the average reconstruction-interval del index $\bar{I}_\delta$ as normally-distributed about a linear transformation of the shift in climatological moisture conditions:

$$\overline{I_\delta^P} | \Delta M \sim N(a_R + b_R \Delta M, \sigma_R^2). \quad (15)$$

The parameters a_R, b_R, and σ_R^2 are fit using calibration-interval data; full model details are given in the supplementary documentation. We adopt an empirical Bayes approach with respect to the parameters of this data-level model and hold them fixed in the reconstruction. The informed prior $[\boldsymbol{\theta}_W | D_{cal}]$ is computed in an offline step using the approach of Tolwinski-Ward et al. (2013).

4.2 Results

Comparing reconstructions constrained by isotope data only, tree-ring data only, and both data sources showcases the relative strengths of each, as well as the power of combining them. When the less informative 7 °C prior is used, the isotope data greatly reduce uncertainty relative to the prior, estimating greater soil moistures than the calibration interval, but do not inform temperature at all (Fig. 6a), which is to be expected given the data-level model independence from ΔT. The ring-width data alone rule out the analogs of response regions I and IV from Fig. 2 in bivariate climate change space; that is, climatologies in which typical years would result in no growth or complacent growth are not given significant posterior probability mass (Fig. 6b). Rather, posterior probability mass is distributed along a characteristic nonlinear

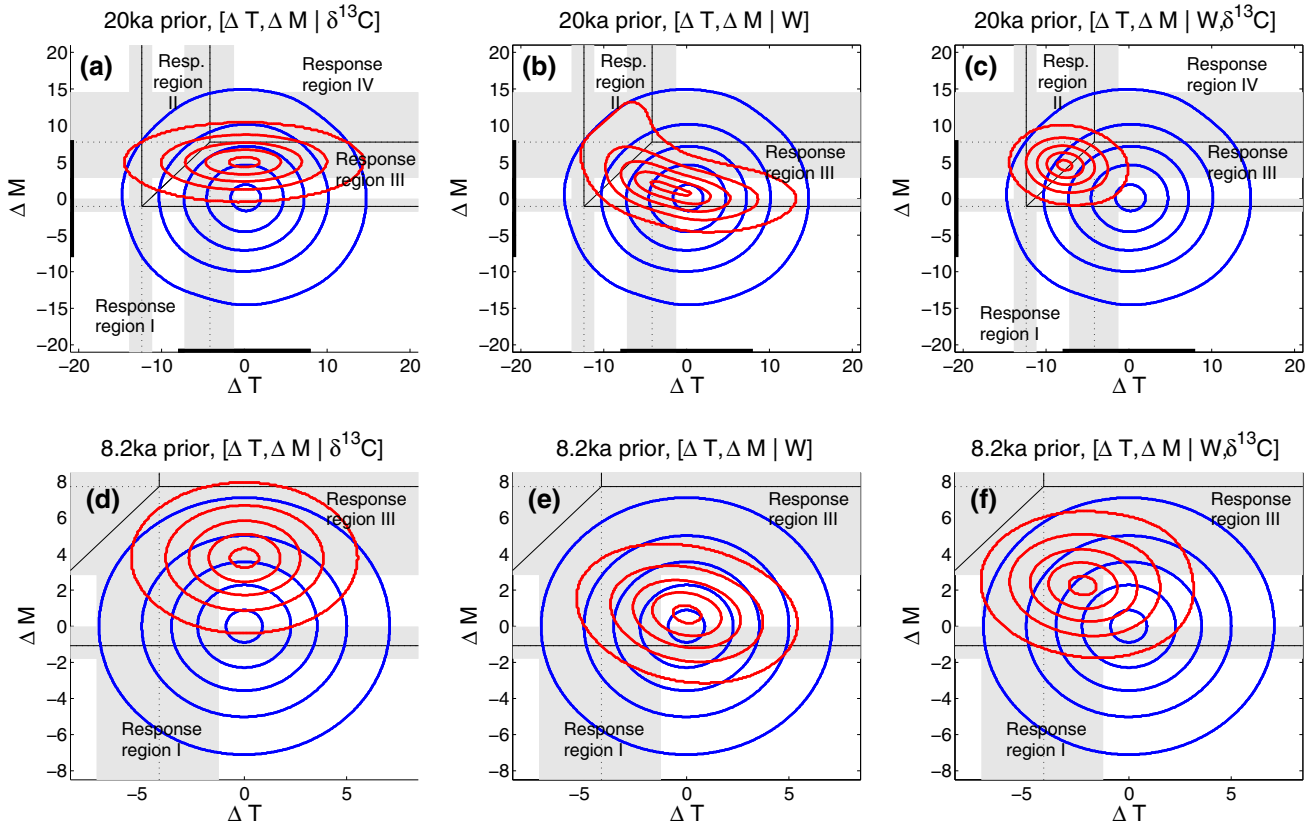

Fig. 6 Contours containing 95, 75, 50, 25, and 5 % of the marginal prior and posterior probability density for ΔT and ΔM at the Methuselah walk site using the extremely broad '7 °C' (*top row*) and the sharper '2.2 °C prior' (*bottom row*). Note the change in scale between rows. **a** and **d** Prior (*blue*) and posterior (*red*) conditioned on isotope data only; **b** and **e** posterior conditioned on tree-ring-width data only; **c** and **f** posterior conditioned on both isotope and ring-width data. *Black bars* along the axes in **a**–**c** show the scale of the axes in **d**–**f**. *Solid black lines* show boundaries of the response regions defined by the posterior medians of the VS-Lite growth response parameters; the *parallel shading* denotes the 95 % credible intervals for these parameters

"boomerang" shape that reflects the nonidentifiability of the tree-ring formation process as described by VS-Lite. Combining both data sources results in the greatest reduction of uncertainty, with the relatively narrow spread in the posterior compared to either single-source paleodata reconstruction indicating a complementarity of the two data sources (Fig. 6c). The multiproxy posterior probabilities of the reconstruction interval controls on tree-ring growth falling into our previously defined classifications, given both data sources and the uncertainty in the estimates of the VS-Lite parameters, are 70 % in the temperature-limited category, 22 % in the moisture-limited category, 0.2 % in the complacent category, and 0 % experiencing no growth at all. The remainder of the probability is allocated to shifts in climatology located close to the "corner" between regions II and III and that yield a mixture of temperature and moisture controls on growth from year to year. Thus under the '7 °C prior', which provides relatively little external constraint, there is a 88 % chance of different climatic controls on growth during the reconstruction interval than those observed during the calibration interval.

The more informative 2.2 °C prior rules out a priori the placement of probability mass near the boundary between regions II and III, and thus posteriors from uniproxy and multiproxy sources show the reconstruction interval climatology still firmly in the linear moisture-sensitive response regime of the trees (Fig. 6d–f). As with the 7 °C prior, conditioning on only the isotope data results in higher estimates of the soil moisture climatology than compared to the calibration interval (Fig. 6d). The posterior given the ring-width data only also shows a tendency toward wetter conditions, as well as some negative association between shifts in temperature and moisture climatology (Fig. 6e). Combining both data sources again results in the greatest reduction of uncertainty (Fig. 6f) with estimated probabilities of the various growth regimes are 0.002 % for temperature-limited, 91.9 % moisture-limited, 8.091 % complacent, and 0 % for climate regimes that are inhospitable for growth. The probability of a change in tree growth controls is estimated in this case to be 8.1 %.

Combined with either prior, the information contained in the isotope and ring-width data together indicate that local conditions were most likely wetter and cooler from 1080–1129 C.E. at the Methuselah Walk site than instrumentally observed modern climates. However, the magnitude of the inferred change, as well as the most likely control on tree-ring growth, depends critically on the choice of prior.

5 Discussion and conclusions

Mechanisms-based forward models of paleodata formation can account for scientifically-understood complexities of data formation, but may result in statistical nonidentifiability in reconstructions of past climate. Using VS-Lite to perform the reconstruction, which provides a more nuanced model of the relationship of tree-ring growth to climate than linear functions of univariate climate, produces bimodality in posterior estimates of temperature and soil moisture. This feature of the posterior accurately reflects the nature of the information contained in the data and the understanding of tree ring formation as modeled by VS-Lite. Without regularization (i.e., additional sources of information), the paleo-observations provide only weak constraints on the solution and cannot distinguish between a set of reconstructed climate histories where past temperature variability explains the observed time series of ring width index, versus a set where moisture variations controlled growth. In situations where no further information exists, and where the data-level model provides the best possible description of the link between the climate and the data, such ambiguity should in fact characterize the most defensible inference that can be drawn from the available information.

Our results also demonstrate two avenues for regularizing such nonidentifiability: complementary paleodata sources, and increasing the information in the prior. The value of a second data source is most clearly demonstrated by comparing posteriors given the various combinations of data under the '7 °C prior'. The posterior uncertainty given either data source alone is large compared to the uncertainty when the two data sets are used for combined inference (Fig. 6a–c). The potential of the prior to regularize the solution is illustrated by comparing the posterior of climatological shifts given tree-ring data using the extremely broad '7 °C prior' versus the much sharper '2.2 °C' prior. If one believes that shifts in the underlying climatology of the magnitude spanned by the former prior were feasible within the reconstructed interval, then one would have to accept that the data could potentially reflect variations in temperature or moisture (Fig. 6b). This degeneracy in the solution is regularized by using the more informative '2.2 °C prior', which transfers the information in the data to posterior inference on moisture conditions, rather than temperature, with nearly absolute certainty (Fig. 6e).

This dependence of the results on the prior underscores the importance of careful prior elicitation. While some argue that priors should contain as little information as possible, if any, so that the data can "speak for themselves", we note that natural paleoclimatic data generally provide only very weak constraints to estimates of past climates precisely because of the complexities of the processes by which they are formed. This feature of the data necessitates informative priors in a paleoclimatic estimation context. Empirical–statistical reconstruction methods

may arrive at the same conclusions as Bayesian analyses by making traditional assumptions *implicitly* before beginning an inference procedure. For example, such methods usually assume the relationship of climate to paleo-observation has not changed in the past, in contrast to the more general and scientifically-grounded data-level model used here. Additionally it is typically assumed that the amplitude of climatic variability captured by the data is contained in the range of instrumentally observed observations, which is analogous to an explicit assumption of a narrower prior in the Bayesian context. We argue that the explicit manner in which assumptions are laid out under the Bayesian framework provides greater transparency under which reconstruction approaches can be critically evaluated and improved as new understanding of climate processes and natural paleoclimate data become available.

The inference that the interval 1080–1129 C.E. was wet and cool at Methuselah Walk relative to the modern record is robust to the choice of prior when the analysis is conditioned on both types of paleodata, and is also consistent with several other lines of evidence. Stine (1990, 1994) used a combination of radiocarbon-dated and precisely located tufa-encrusted plant remains and geomorphic features to demonstrate the existence of 'extremely severe drought conditions for more than two centuries before AD 1112 and for more than 140 years before AD 1350' in this part of California, including Mono Lake, a basin with no outlet. Stine (1990, 1994) also noted that, between the two droughts, there was a 'period of increased wetness' in the eastern Sierra Nevada that resulted in a high stand of Mono Lake that has only been surpassed twice since, in the late fifteenth and mid seventeenth centuries C.E. (Stine 1990, Fig. 6). Subsequently, Graham and Hughes (2007) used hydrologic modeling to quantitatively link moisture-sensitive tree-ring width records in the White Mountains to Mono Lake level. Reconstructions of North American megadroughts from tree-ring networks by Cook et al. (2009) also find our interval to be comparably moist, while temperature reconstructions of LaMarche (1974) and Salzer et al. (2009, 2013) further support the inference of cooling conditions throughout the late eleventh/early twelfth century.

There are several ways the present model could be expanded for future applications. In the presence of more data, the inference could be made fully Bayesian, with all modeling parameters inferred rather than estimated and held fixed as we have done here. The priors on the process-level parameters ΔT and ΔM could also be made more informative given process-based understanding of the co-variability and relative magnitude of likely lower-frequency changes in temperature and moisture at a given location. The development of a spatial extension of the current hierarchical model would enable the reconstruction of spatially explicit fields of covarying temperature and soil moisture given continental-scale networks of tree-ring width. Even without the expensive estimation of high-dimensional subannual climatic variations, such a scheme would be valuable for allowing probabilistic attribution of changes in ring-width mean and variance across networks of dendrochronologies to shifts in one of temperature, moisture, or a combination of both, while accounting for potential differences in the climatic controls on tree growth through time. This could be especially interesting during fixed temporal intervals of climatological interest, such as the Little Ice Age or Medieval Climate Anomaly. Independent data sources that constrain past climate with relative certainty, such as the extensive documentary records in Europe (Brazdil et al. 2005; Luterbacher et al. 2004), could be integrated into a hierarchical model that contains a VS-Lite data level in order to assess the probability of pre-instrumental changes in the response of tree-ring data in the same spatial domain.[3] While our model for the observed data at Methuselah Walk accounts for some of the complexities in ring-width formation, a forward model of isotope fractionation, such as that by Farquhar et al. (1982), could be used to incorporate mechanistic understanding of the isotope signal formation, and take account of the second-order effects of temperature and sunlight on the data series and the uncertainty they induce in the reconstructed climate.

Finding candidate ring-width series for this study whose signal might be affected by interactions between low frequency climate variability and biological growth thresholds was a challenge. While this meta-result could indicate that this kind of switching is unlikely to occur in nature, it could also be interpreted as testimony to the techniques developed by dendroclimatologists to sample trees that are likely to contain a univariate signal. The carefully-selected samples are therefore unlikely to be near the boundaries of the different regions of response space depicted in Fig. 2. Indeed, our reconstruction using the more conservative '2.2 °C prior' and both sources of paleoproxy data lend support to the use of the uniformitarian principle in the case of the Methuselah Walk site, as tree growth appears to be solidly moisture limited even for relatively large changes in the background climate. Samples that do sit close to the biological margins for signal switching may also be unlikely to make their way into the literature, because they will be necessarily more difficult to interpret within the established framework of univariate response functions. Our method provides a means to broaden the set of sampled trees from which useful climatic information might be derived. It may also be of use in diagnosing genuine departures from linear tree growth responses to climate.

[3] Werner, J.P. and Tolwinski-Ward, S.E., poster PP51A-1913 of the American Geophysical Union Fall Meeting (2013).

While incorporating the nonlinear response to two interacting variables makes our hierarchical model more complex than traditional linear-empirical models, the VS-Lite data level neglects many other real-world complexities of tree growth. Indeed, potential switching in growth response between temperature controls and moisture controls is only one of many mechanisms by which a tree's response to climate can change over time, including changes in the timing of snowmelt (Vaganov et al. 1999), the effects of changes in solar radiation on photosynthesis (Stanhill and Cohen 2001), and end effects in the statistical detrending of ring-width series (D'Arrigo et al. 2004). Still, the present study gives a flavor of the statistical challenges that can arise as increasingly complex models of data formation are used to interpret paleoobservations in the inverse reconstruction context. Our results suggest that mechanistic-statistical Bayesian hierarchical modeling approaches may be most useful for climate reconstructions where researchers have either a strong hypothesis for the type of nonlinearity that may complicate the data, or else more data sources that can help constrain the likely state space.

Acknowledgments This work was supported in part by Grants NSF ATM-0724802, NSF ATM-0902715, NSF DMS-1204892, NSF AGS 1304309, and NOAA NA060OAR4310115. We thank Steve Leavitt for lending his isotope data as well as insights on their interpretation, Chris Daly and the PRISM project for making their work freely available, and Benno Blumenthal for making the PRISM data easily accessible on the IRI Data Library. We are also grateful for insightful comments from Chris Paciorek and one other anonymous reviewer, which substantially improved the final version of this paper.

Appendix: Sampling algorithm

Posterior sampling is complicated by the many-to-one mapping from climate to tree-ring width inherent to the VS-Lite model. As a result, it is usually possible to construct many hot, dry moisture-limited climate histories as well as many cool, wet temperature-limited ones with the same likelihood from a given series of interannaul ring-width variations. The nonidentifiability between hot and dry solutions versus cool and wet solutions is related to the switching in the controls on tree-ring growth that can occur with large shifts in the low-frequency climatology, and results in bimodality in the posterior distribution of ΔT and ΔM. This feature of the problem precludes the use of standard Gibbs sampling approaches, in which each variable in the problem is iteratively sampled from its full conditional given the current value of all others unknowns (Gilks et al. 1996). Fixed values of the (2-variable $\times$ 12-month $\times$ N-year) histories of climatic anomalies $\boldsymbol{T}', \boldsymbol{M}'$ will only be consistent with either a hot, dry climate and moisture-limited growth, or with a cool, wet climate and temperature-limited growth, and so a straightforward Gibbs sampler does not permit transitions between the two modes of the posterior of ΔT and ΔM. The posterior is of the "doubly intractable" form discussed by Murray et al (2006).

Further nonidentifiability stems from the finer time-scale of the monthly climatic variations compared to the annual resolution of the data, as there are many ways to configure monthly climate variations resulting in the same annual growth. Thus, for a given shift in climatology captured by non-zero values of ΔT and ΔM, and conditional on the parameters of VS-Lite controlling the growth response, a relatively long "burn-in" period is necessary to wander through the (2-variable $\times$ 12-month $\times$ N-year) space of $\boldsymbol{T}', \boldsymbol{M}'$ histories to find the region of state space that is statistically consistent with both the data and the prior.

Given these complications, we employ a hybrid of Gibbs and Metropolis–Hastings sampling techniques, as well as an approximation of the likelihood using summary statistics and simulation as in Approximate Bayesian Computation approaches (Csillery et al. 2010) to numerically estimate the posterior. The approximation to the likelihood is based on the following intuition: variations in the climatological shifts $(\Delta T, \Delta M)$ tend to influence the mean and variance of simulated tree-ring width time series, while the climatic anomalies T', M' mainly control the relative interannual variations in ring width index. By treating the ring-width series as a set of variations about its sample mean with scale given by the sample standard deviation, and by treating the sample mean and variance as sufficient statistics for ΔT and ΔM, we can solve an approximation to the problem, with the likelihood in Eq. 11 approximated by

$$\begin{aligned}[\boldsymbol{W}|\boldsymbol{T}', \boldsymbol{M}', \Delta T, \Delta M] &= [\boldsymbol{W}', \bar{W}, s_W^2|\boldsymbol{T}', \boldsymbol{M}', \Delta T, \Delta M] \\ &\approx [\boldsymbol{W}'|\boldsymbol{T}', \boldsymbol{M}'][\bar{W}, s_W^2|\Delta T, \Delta M]\end{aligned} \quad (16)$$

The sampling for the pseudoproxy problem then proceeds in two separate steps:

1. Draw a proposal from the prior $[\Delta T, \Delta M]$, and a Monte Carlo sample of size 100 from $[\boldsymbol{T}', \boldsymbol{M}']$ (sampled from Eq. 9 using the fixed values of covariance matrices S_s and temporal autocorrelation parameters ϕ_1 and ϕ_2 estimated in the calibration interval). Use these as inputs to the data-level model Eq. 6 to compute a Monte Carlo sample $\{\bar{W}_{MC}, S^2_{MC}\}_{n=1}^{100}$ of the sample mean and standard deviation of the simulated ring-width index time series. Accept or reject the proposed values of $\Delta T, \Delta M$ (as in a Metropolis–Hastings sampler) depending on the distance of the Monte Carlo sample means of the two sample statistics from the observed values. The likelihood is a normal

distribution of the means of the Monte Carlo sample statistics about the observed values, with standard deviations given by the Monte Carlo standard errors. We run this step in series on a laptop. The resulting samples $\{\Delta T^{(n)}, \Delta M^{(n)}\}_{n=1}^{N}$ approximate the distribution $[\Delta T, \Delta M|\bar{W}, s_W^2] \approx [\Delta T, \Delta M|\boldsymbol{W}]$.

2. Using the Metropolis–Hastings within Gibbs algorithm (Gilks et al. 1996), draw $n = 1, \ldots, N_{MC}$ samples of the monthly-resolved bivariate time series from

$$[\boldsymbol{T}', \boldsymbol{M}'|\Delta T^{(n)}, \Delta M^{(n)}, \boldsymbol{W}] \propto [\boldsymbol{W}|\boldsymbol{T}', \boldsymbol{M}', \Delta T^{(n)}, \Delta M^{(n)}][\boldsymbol{T}', \boldsymbol{M}']$$

for each of the samples of the climatic shifts from Step 1, where the first factor on the right-hand side is given by our VS-Lite data-level model, and the second is given by the prior model (Eq. 9) for the climatic anomalies. We use a burn-in period of 75 iterations, which was deemed appropriate after diagnosis of multiple MCMC chains examining trace plots, autocorrelation plots, and the $\hat{R}$ statistic of Gelman and Rubin (1992) for our sample chains. We parallelize this step and draw the samples in a high-performance computing (HPC) environment.

The sampler for the reconstructions based on real tree-ring data at Methuselah walk proceeds similarly, except that $\boldsymbol{\theta}_W$ must also be inferred. Because the elements of $\boldsymbol{\theta}_W$ depend only on calibration-interval temperature, moisture, and ring-width data $(\boldsymbol{W}_c, \boldsymbol{T}_c, \boldsymbol{M}_c)$, this sampling can be performed separately, and we draw samples from $[\boldsymbol{\theta}_W|\boldsymbol{W}_c, \boldsymbol{T}_c, \boldsymbol{M}_c]$ using the algorithm and freely available code detailed in Tolwinski-Ward et al. (2013). The likelihoods in Steps 1 and 2 also depend, in the real-data reconstructions, on the sampled values of $(\boldsymbol{\theta}_w, \boldsymbol{W}_c, \boldsymbol{T}_c, \boldsymbol{M}_c)$, which serve as inputs to VS-Lite. For inference conditioned on both tree-ring width and isotope data, the dependence of the sampler on the isotopes enters during the drawing of proposals for the Metropolis–Hastings sampler in Step 1, by drawing proposals of ΔM conditional on the mean del-index $\bar{I}_\delta$.

All sampling was coded and run in MATLAB®. The CPU time for each step and each experiment is given in the Table 2.

Table 2 Computing time for sampling

	Pseudoproxy experiment (2,000 draws thinned from 20,000)	Methuselah walk reconstruction (10,000 draws thinned from 100,000)
Step 1	~2 CPU hours (laptop)	~10 CPU hours (laptop)
Step 2	~21 CPU hours (HPC)	~350 CPU hours (HPC)

References

Bale R, Robertson I, Salzer M, Loader N, Leavitt S, Gagen M, Harlan T, McCarroll D (2011) An annually resolved bristlecone pine carbon isotope chronology for the last millennium. Quatern Res 76(1):22–29. doi:10.1016/j.yqres.2011.05.004

Bradley R (1999) Paleoclimatology: reconstructing climates of the quaternary. Academic Press, San Diego, CA

Bradley R (2011) High-resolution paleoclimatology. In: Hughes M, Swetnam T, Diaz H (eds) Dendroclimatology: progress and prospects, developments in paleoecological research, Chapter 1. Springer, Berlin

Brazdil R, Pfister C, Wanner H, Von Storch H, Luterbacher J (2005) Historical climatology in Europe: the state of the art. Clim Change 70:363–430. doi:10.1007/s10584-005-5924-1

Breitenmoser P, Brönnimann S, Frank D (2013) Forward modelling of tree-ring width and comparison with a global network of tree-ring chronologies. Clim Past Discuss 9(4):4065–4098. doi:10.5194/cpd-9-4065-2013. http://www.clim-past-discuss.net/9/4065/2013/

Chiles J, Delfiner P (1999) Geostatistics: modeling spatial uncertainty. Wiley Series in Probability and Statistics, New York, NY

Christiansen B, Ljungqvist F (2011) Reconstruction of the extratropical NH mean temperature over the last millennium with a method that preserves low-frequency variability. J Clim 24:6013–6034. doi:10.1175/2011JCLI4145.1

Cook E, Kairiukstis L (1990) Methods of Dendrochronology: applications in the environmental sciences. Kluwer Academic Publishers, Dordrecht

Cook E, Seager R, Heim R, Vose R, Herweijer C, Woodhouse C (2009) Megadroughts in North America: placing IPCC projections of hydroclimatic change in a long-term paleoclimate context. J Quat Sci 25:48–61. doi:10.1002/jqs.1303

Crowley T, Lowery T (2000) How warm was the medieval warm period? AMBIO 29:51–54. doi:10.1639/0044-7447(2000

Csillery K, Blum M, Gaggiotti O, Fracois O (2010) Approximate Bayesian computation (ABC) in practice. Trends Ecol Evol 25:410–418. doi:10.1016/j.tree.2010.04.001

Daly C, Halbleib M, Smith J, Gibson W, Doggett M, Taylor G, Curtis J, Pasteris P (2008) Physiographically sensitive mapping of climatological temperature and precipitation across the coterminous United States. Int J Climatol 28:2031–2064. doi:10.1002/joc.1688. http://www.prism.oregonstate.edu/

D'Arrigo R, Kaufmann R, Davi N, Jacoby G, Laskowski C, Myneni R, Cherubini P (2004) Thresholds for warming-induced growth decline at elevational treeline in the Yukon Territory. Glob Biogeochem Cycles 18. doi:10.1029/2004GBO02249

D'Arrigo R, Wilson R, Jacoby G (2006) On the long-term context for late twentieth century warming. J Geophys Res 111. doi:10.1029/2005JD006352

Evans M, Tolwinski-Ward S, Thompson D, Anchukaitis K (2013) Applications of proxy system modeling in high resolution paleoclimatology. Quat Sci Rev 76(0):16–28. doi:10.1016/j.quascirev.2013.05.024. http://www.sciencedirect.com/science/article/pii/S0277379113002011

Farquhar G, O'Leary MH, Berry JA (1982) On the relationship between carbon isotope discrimination and the intercellular carbon dioxide concentration in leaves. Aust J Plant Physiol 9:121–37

Fritts HC (2001) Tree rings and climate. The Blackburn Press, New York

Fritts HC, Smith DG, Cardis JW, Budelsky C (1965) Tree-ring characteristics along a vegetation gradient in northern Arizona. Ecology 46:394–401. http://www.jstor.org/stable/1934872

Garetta V, Guiot J, Mortier F, Chadoef J, Hely C (2012) Pollen-based climate reconstruction: calibration of the vegetation–pollen

processes. Ecol Mod 235–236:81–94. doi:10.1016/j.ecolmodel.2012.03.031
Gelman A, Rubin D (1992) Inference from iterative simulation using multiple sequences. Stat Sci 7(4):457–472. doi:10.1214/ss/1177011136
Gelman A, Carlin J, Stern H, Rubin D (2003) Bayesian data analysis. Chapman and Hall, Boca Raton, FL
Gilks W, Richardson S, Spiegelhalter D (1996) Markov chain Monte Carlo in practice. Chapman & Hall/CRC, Boca Raton
Graham N, Hughes M (2007) Reconstructing the Mediaeval low stands of Mono Lake, Sierra Nevada, California USA. Holocene 17(8):1197–1210. doi:10.1177/0959683607085126
Guiot J, Torre F, Jolly D, Peyron O, Boreaux J, Cheddadi R (2000) Inverse vegetation modeling by monte carlo sampling to reconstruct palaeoclimates under changed precipitation seasonality and CO2 conditions: application to glacial climate in Mediterranean region. Ecol Model 127:119–1140
Guiot J, Wu V Garreta, HB, Hatte C, Magny M (2009) A few prospective ideas on climate reconstruction: from a statistical single proxy approach towards a multi-proxy and dynamical approach. Clim Past 5:571–583. www.clim-past.net/5/571/2009/
Haslett J, Whiley M, Bhattacharya S, Salter-Townshend M, Wilson S, Allen J, Huntley B, Mitchell F (2006) Bayesian paleocolimate reconstruction. J R Stat Soc 169(3):395–438. doi:10.1111/j.1467-985X.2006.00429.x
Huang J, van den Dool HM, Georgankakos KP (1996) Analysis of model-calculated soil moisture over the United States (1931–1993) and applications to long-range temperature forecasts. J Clim 9:1350–1362
Hughes M, Funkhouser G (1998) Extremes of moisture availability reconstructed from tree rings for recent millennia in the Great Basin of Western North America. In: Beniston M, Innes J (eds) The impacts of climate variability on forests. Springer, Berlin, pp 99–107
Hughes MK, Ammann CM (2009) The future of the past: an earth system framework for high resolution paleoclimatology—editorial essay. Clim Change 94:247–259. doi:10.1007/s10584-009-9588-0
Jansen E, Overpeck J, Briffa K, Duplessy J, Joos F, Masson-Delmotte V, Olago D, Otto-Bliesner B, Peltier W, Rahmstorf S, Ramesh R, Raynaud D, Rind D, Solomina O, Villalba R, Zhang D (2007) Paleoclimate, Chap 6. In: Solomon S, Qin D, Manning M, Chen Z, Marquis M, Averyt K, Tignor M, Miller H (eds) Climate change 2007: the physical science basis. Contribution of working group I to the fourth assessment report of the intergovernmental panel on climate change. Cambridge University Press, Cambridge
Jones P, Briffa K, Barnett T, Tett S (1998) High-resolution paleoclimatic records for the last millennium: interpretation, integration and comparison with general circulation model control-run temperatures. Holocene 8:455–471. doi:10.1191/095968398667194956
Kobashi T, Severinghaus JP, Brook EJ, Barnola JM, Grachev AM (2007) Precise timing and characterization of abrupt climate change 8200 years ago from air trapped in polar ice. Quat Sci Revs
LaMarche V (1974) Paleoclimatic inferences from long tree-ring records. Science 183(4129):1043–1088
Leavitt S (1994) Major wet interval in White Mountains medieval warm period evidenced in δ^{13}C of bristlecone pine tree rings. Clim Change 26:299–307
Li B, Nychka D, Ammann C (2010) The value of multiproxy reconstructions of past climate. J Am Stat Assoc 105(491):883–895
Luterbacher J, Dietrich D, Xoplaki E, Grosjean M, Wanner H (2004) European seasonal and annual temperature variability, trends, and extremes since 1500. Science 303(5663):1499–1503. doi:10.1126/science.1093877
Mann ME, Zhang Z, Hughes MK, Bradley RS, Miller SK, Rutherford S, Ni F (2008) Proxy-based reconstructions of hemispheric and global surface temperature variations over the past two millennia. Proc Natl Acad Sci USA 105:13,252–13,257. doi:10.1073/pnas.0805721105
McCarroll D, Loader N (2004) Stable isotopes in tree rings. Quat Sci Rev 23:771–801. doi:10.1016/j.quascirev.2003.06.017
Moberg A, Sonechkin D, Holmgren K, Datsenko N, Karlen W (2005) Highly variable Northern Hemisphere temperatures reconstructed from low- and high-resolution proxy data. Nature 433:613–617. doi:10.1038/nature03265
Murray I, Ghahramani Z, MacKay DJC (2006) MCMC for doubly-intractable distributions. In:Proceedings of the 22nd Annual Conference on Uncertainty in Artificial Intelligence (UAI-06), pp 359–366
Parnell A, Haslett J, Allen J, Buck C, Huntley B (2008) A flexible approach to assessing synchroneity of past events using Bayesian reconstructions of sedimentation history. Quat Sci Rev 27(19–20):1872–1885. doi:10.1016/j.quascirev.2008.07.009
Robert C (2007) The bayesian choice: from decision-theoretic foundations fo computational implementation. Springer Texts in Statistics, Paris
Salzer M, Bunn A, Graham N, Hughes M (2013) Five millennia of paleotemperature from tree-rings in the Great Basin, USA. Clim Dyn 1–10. doi:10.1007/s00382-013-1911-9
Salzer MW, Hughes MK, Bunn AG, Kipfmueller KF (2009) Recent unprecedented tree-ring growth in bristlecone pine at the highest elevations and possible causes. Proc Natl Acad Sci USA 106:20,348–20,353. doi:10.1073/pnas.0903029106
Shashkin A, Vaganov E (1993) Simulation model of climatically determined variability of conifers annual increment (on the example of common pine in the steppe zone). Rus J Ecol 24(5):275–280
Smerdon J (2012) Climate models as a test bed for climate reconstruction methods: pseudoproxy experiments. WIREs Clim Change 3:63–77. doi:10.1002/wcc.149
Stanhill G, Cohen S (2001) Global dimming: a review of the evidence for a widespread and significant reduction in global radiation with discussion of its probable causes and possible agricultural consequences. Agric For Meteorol 107:255–278. doi:10.1016/S0168-1923(00)00241-0
Stine S (1990) Late Holocene fluctuations in Mono lake, eastern California. Paleogeography, paleoclimatology, palaeoecology 78:333–381. doi:10.1016/0031-0182(90)90221-R
Stine S (1994) Extreme and persistent drought in California and Patagonia during Mediaeval time. Nature 369:546–549. doi:10.1038/369546a0
Stokes M, Smiley T (1968) An introduction to tree-ring dating. University of Chicago Press, Chicago
Tingley M, Huybers P (2010a) A Bayesian algorithm for reconstructing climate anomalies in space and time. Part I: development and applications to paleoclimate reconstruction problems. J Clim 23:2759–2781. doi:10.1175/2009JCLI3015.1
Tingley M, Huybers P (2010b) A Bayesian algorithm for reconstructing climate anomalies in space and time. Part II: comparison with the regularized expectation-maximization algorithm. J Clim 23:2782–2800. doi:10.1175/2009JCLI3016.1
Tingley M, Huybers P (2013) Recent temperature extremes at high northern latitudes unprecedented in the past 600 years. Nature 496(7444):201–205. doi:10.1038/nature11969
Tingley M, Craigmile P, Haran M, Li B, Mannshardt-Shamseldin E, Rajaratnam B (2012) Piecing together the past: statistical insights into paleoclimatic reconstructions. Quat Sci Rev 35:1–22. doi:10.1016/j.quascirev.2012.01.012

Tolwinski-Ward S, Evans M, Hughes M, Anchukaitis K (2011) An efficient forward model of the climate controls on interannual variation in tree-ring width. Clim Dyn doi:10.1007/s00382-010-0945-5

Tolwinski-Ward S, Anchukaitis K, Evans M (2013) Bayesian parameter estimation and interpretation for an intermediate model of tree-ring width. Clim Past 9:1481–1493. doi:10.5194/cp-9-1481-2013

Vaganov E, Hughes M, Kirdyanov A, Schweingruber F, Silkin P (1999) Influence of snowfall and melt timing on tree growth in subarctic Eurasia. Nature 400:149–151. doi:10.1038/22087

Vaganov E, Hughes M, Shashkin A (2006) Growth dynamics of conifer tree rings: images of past and future environments. Springer Ecol. Stu. 183, New York

Wahl E, Diaz H, Ohlwein C (2011) A pollen-based reconstruction of summer temperature in central North America and implications for circulation patterns during medieval times. Glob Planet Change. doi:10.1016/j.gloplacha.2011.10.005

Yu S, Kang Z, Zhou W (2012) Quantitative palaeoclimate reconstructions as an inverse problem: A Bayesian inference of late-Holocene climate on the eastern Tibetan Plateau from a peat cellulose $\delta^{18}O$ record. Holocene 22(405). doi:10.1177/0959683611425544